

Droplet Phenomenology and Mean Field in a Frustrated Disordered System

J. Houdayer and O. C. Martin

Division de Physique Théorique, Institut de Physique Nucléaire, Université Paris-Sud, F-91406 Orsay Cedex, France.

(May 1, 2018)

The low lying excited states of the three-dimensional minimum matching problem are studied numerically. The excitations' energies grow with their size and confirm the droplet picture. However, some low energy, infinite size excitations create multiple valleys in the energy landscape. These states violate the droplet scaling ansatz, and are consistent with mean field predictions. A similar picture may apply to spin glasses whereby the droplet picture describes the physics at small length scales, while mean field describes that at large length scales.

75.10.Nr, 64.60.Cn, 02.60.Pn

A most useful approach in the study of disordered systems is the replica method. It has been successfully applied [1] to the Sherrington and Kirkpatrick (SK) model [2] of spin glasses, yielding exact results and revealing remarkable properties such as multiplicity of nearly degenerate ground states, lack of self-averaging, and ultrametricity. However it is not clear whether these “mean field” properties hold for more realistic spin glass models like the one of Edwards and Anderson [3] where finite dimensional effects may be dominant. To tackle systems in finite dimensions, a number of approaches based on scaling and the renormalization group have been proposed [4–6]. In these phenomenological pictures, it is assumed that there is a unique ground state (up to a global symmetry) and that excitation energies satisfy a scaling ansatz. For our purposes, the essential ingredient of this ansatz is that a “droplet”, defined as the lowest energy excitation of characteristic size L containing a given spin, is assumed to have an energy which scales as L^θ , with $\theta > 0$. Hereafter we refer to such approaches as the “droplet picture”.

Although the “mean field” and droplet pictures are very different, they both agree that there are numerous local minima in the energy landscape separated by significant energy barriers. The corner-stone of disagreement between the two approaches concerns the energy of excitations whose size is comparable to that of the whole system. In the mean field picture, there are such system-size excitations whose excitation energies are finite, *i.e.*, do not grow with the system size. Thus there are many nearly degenerate ground states and the energy landscape consists of numerous similar low energy valleys. On the contrary, in the droplet picture, the characteristic energy for such system-size excitations grows as a positive power of the size of the system. As a conse-

quence, the probability of having such an excitation with an energy below a fixed value goes to zero as the system size grows. Thus the ground state is almost never nearly degenerate with another significantly different local minimum. Furthermore, from the point of view of the droplet scaling ansatz, the existence of many nearly degenerate ground states would lead to $\theta \leq 0$, and yet, for the spin glass phase to exist at non-zero temperatures, droplet excitations must be suppressed, leading to $\theta > 0$.

These points show that an unambiguous determination of the lowest energies of large scale excitations would help resolve the controversy over the relevance of the droplet and mean field pictures to finite dimensional spin glasses. Unfortunately, the main obstacle in the way of such a test is the computational complexity of spin glasses: just finding the ground state is *NP*-hard [7], and finding the excited states is at least as demanding computationally. We have thus chosen to investigate a different system: the three-dimensional minimum matching problem (see below). Although it is both frustrated and disordered, it is computationally more tractable than a spin glass. For this system we have devised a new algorithm which allows us to enumerate very efficiently *all* the states above the ground state in a systematic way. To our knowledge, this is the first time it is possible to explore unambiguously a non-trivial frustrated disordered model. With our computational tool and some analysis, we find that the droplets in this model have energies which grow with their size, justifying a droplet picture with a positive exponent θ . However we also find that the thermodynamic limit is a bit singular. In particular, some “infinite” size droplets appear at low energies, creating an energy landscape with many nearly degenerate valleys. Our three-dimensional model thus has a droplet like behavior at finite length scales, but its energy landscape at large length scales is as predicted by mean field.

The model — We consider a system arising in combinatorial optimization: the minimum matching problem (MMP) [7]. This choice is motivated by the following properties: (i) the problem of finding ground states of two-dimensional spin glasses can be mapped to a MMP [8] (see [9] for recent developments); (ii) we are able to compute quickly and exactly the ground state *and* the excited states of the MMP for any realization of the disorder; (iii) a droplet picture can be constructed quite naturally; (iv) the replica approach has been used to solve a mean field approximation of the model [10].

Consider N points (N even) and the set of “distances” between them. These distances define the instance, that

is the quenched disorder. A micro-state or configuration is any “matching” of the points, that is a dimerization, so that each and every point is paired with exactly one other point. The energy of a matching is defined as the sum of the distances between matched points. The MMP, as defined in combinatorial optimization, consists of finding the lowest energy matching. Because of the disorder, the system is frustrated: each point would like to be paired to its nearest neighbor, but in general this cannot be achieved for all points. In the *statistical physics* formulation, one sums over all micro-states, weighting them with the Boltzmann factor. One also takes the thermodynamic limit ($N \rightarrow \infty$), and for that, one must specify the quenched disorder ensemble.

In the Euclidean form of the MMP, one considers N points at random in a 3-dimensional volume. In order to avoid edge effects, we use a cube with periodic boundary conditions. The large N limit is taken at fixed density of points, and thus corresponds to the usual infinite volume limit. (In these units, which we use hereafter, the volume is equal to N and the ground state energy is extensive, *i.e.*, proportional to N .) To tackle this model, it is useful to consider a mean field approximation of the problem; this has been done by Mézard and Parisi [10] who applied replicas to a modified model where all correlations among distances between points were removed. Hereafter, we call this modified model the (independent) *random-link* MMP because all the “distances” between pairs of points are independent random variables. These individual distances are taken to be distributed as in the Euclidean model.

In a parallel with spin glasses, one can consider the Euclidean MMP to be the analogue of the Edwards-Anderson model, incorporating frustration and disorder in a Euclidean space; similarly, the analogue of the SK (or better yet, the Viana-Bray [11]) model is the *random-link* MMP. It is known that the random-link model provides an excellent approximation for the ground state energy density of the Euclidean MMP. (See [12] for an overview of some of the associated properties of ground states.) Now we will see that it also enables one to understand the corresponding energy landscape.

Excitations — A general matching differs from the ground state by replacing some of the bonds by others. One can organize those two sets of bonds into alternating loops where every other bond in a loop belongs to the ground state matching, the others belonging to the excited state matching. (This follows from the fact that each point is matched to one and only one other point; see Figure 1 and [13].) Any excited state thus consists of alternating loops which are non-overlapping, *i.e.*, which have no points in common. The total excitation energy is the sum of the energies of each loop. With this insight, the system can be viewed as an (interacting) gas of loops. Hereafter, we consider only excitation energies, *i.e.*, all energies are measured relative to the ground state

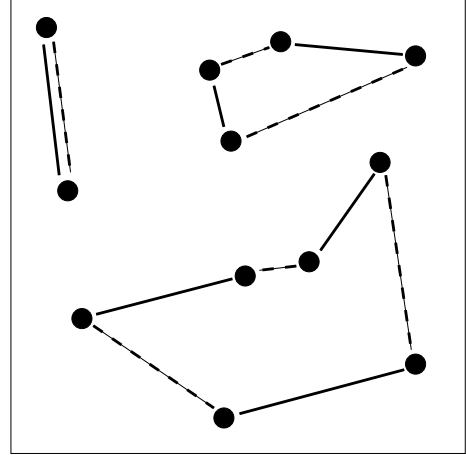


FIG. 1. Comparison of two matchings. One is in solid lines, the other is in dashed lines. Non intersecting alternating loops describe the difference of the two matchings. Here there are two loops, of sizes 4 and 6.

energy. Also, we define the *size* of a loop as the number of bonds it has; the size ℓ of any loop is thus even and satisfies $4 \leq \ell \leq N$.

Local density of states — At low enough temperatures, this gas of loops becomes very dilute, suggesting that “loop-loop” interactions may be neglected (recall that the loops cannot overlap). In this approximation, the thermodynamics of the gas may be computed from the local density of states associated with single loop excitations. Thus we have determined numerically the local density $\rho_\ell(E)$ of one-loop states of size ℓ and of energy E . To accomplish this, for each realization of the disorder, we generate all the single loops up to a maximum energy. Our algorithm does this in a systematic way by successively increasing the length of different bonds and finding the new ground states. This increase in length has the effect of preventing the new ground states from containing certain bonds. The process can be organized into a tree search with a branch and bound so that all the states below a given energy are obtained. We then determine the number $\mathcal{N}_\ell(E)$ of loops of size ℓ with energy between E and $E + \Delta E$. We have averaged $\mathcal{N}_\ell(E)$ over 10^3 to 10^4 randomly generated instances for $N = 50, 100, 150, 200$, and 250 points; this leads to the estimator $\rho_\ell(E) = \langle \mathcal{N}_\ell \rangle / N \Delta E$. Our data show that the different values of N lead to the same function, justifying the definition of $\rho_\ell(E)$ and indicating that our values of N are large enough for finite size effects to be negligible. For each ℓ , we find that $\rho_\ell(E)$ is a smoothly increasing function of E with the property $\rho_\ell(0) \neq 0$. This fact can be understood by considering the measure of the points leading to a loop of zero energy. (It should be clear that finite dimensional spin glasses also have this property because the probability density of having a cluster of spins

TABLE I. Density of states at zero energy as a function of the loop size in the three dimensional Euclidean MMP.

ℓ	$\rho_\ell(0)$	$\ell^2 \rho_\ell(0)$
4	4.520	72.3
6	0.840	30.2
8	0.367	23.5
10	0.205	20.5

in a null local field is non-zero.)

Droplets — Fisher and Huse [6] define droplets in the context of spin glasses; generalizing their definition to the matching problem is straightforward. For a given point, consider the set of all single loops of size ℓ ($L \leq \ell < 2L$) passing through that point. Define the droplet of characteristic size L containing that point as the loop in the defined set with the lowest energy. When applied to the MMP, the droplet picture states that the typical energy of droplets of size L scales as L^θ , $\theta > 0$. Furthermore, the scaling ansatz [6] says that the probability distribution of the energy E_L of a droplet of size L behaves as

$$P_L(E_L) = p(E_L/L^\theta)/L^\theta \quad (1)$$

with $p(0) \neq 0$. A direct test of this scaling ansatz is beyond the possibilities of our numerics because large values of L would require too large computation times. Thus we have instead performed an indirect test of the scaling ansatz as follows.

Our method is based on relating $p(0)$ to the $\rho_\ell(0)$'s. Since we are concerned with very low energies, excitations are rarefied; as in the dilute gas approach, we will assume that the excitations are independent. Using Equation 1, we derive the probability distribution of the lowest energy droplet of size L in the *whole* system, and find that the mean of this distribution is $L^{1+\theta}/Np(0)$. (For this, we assumed that the droplets were independent; we also used the property that the number of droplets of size L is N/L up to constant factors, each droplet containing $O(L)$ points.) We can also calculate this mean using the $\rho_\ell(0)$'s; setting the two expressions to be equal leads to the sum rule

$$\rho_L(0) + \rho_{L+2}(0) \cdots + \rho_{2L-2}(0) = p(0)/L^{1+\theta}. \quad (2)$$

(In the case of spin glasses, the exponent would be $3 + \theta$ assuming that droplets of size L have $O(L^3)$ spins.) If the scaling with $\theta > 0$ is valid, Equation 2 gives $\rho_\ell(0) = O(\ell^{-2-\theta})$. In Table I we give the results for $\rho_\ell(0)$ and $\ell^2 \rho_\ell(0)$ as a function of ℓ for the values of ℓ within reach of our computations. (Our data have statistical errors which prevent us from going to much larger values of ℓ in a meaningful way.) The positivity of θ is confirmed by the decrease of these quantities with increasing ℓ , giving good evidence that the droplet picture applies to the MMP.

Breakdown of the droplet picture — Consider now the distribution $P(\ell_1, N)$ of the length ℓ_1 of the first excited

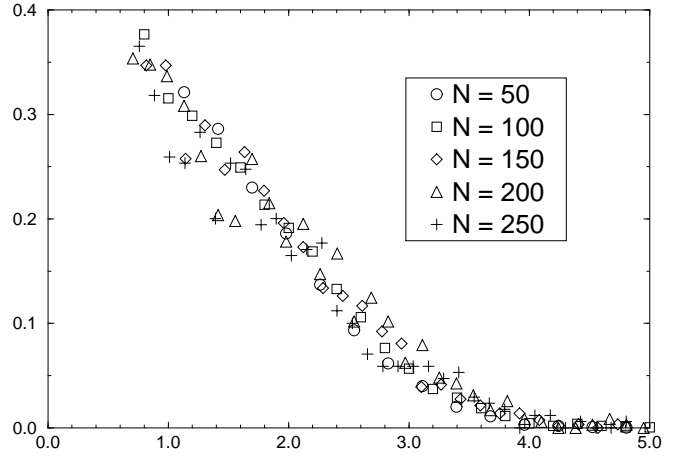


FIG. 2. Scaling function $G(x)$ (see Equation 3) for different values of N .

state. This quantity is easy to extract numerically; furthermore, $P(\ell_1, N)$ is a probability distribution over ℓ_1 , and a calculation similar to the one just discussed gives $P(\ell_1, N) = \rho_{\ell_1}(0) / \sum_{\ell'} \rho_{\ell'}(0)$. When $N \rightarrow \infty$, $P(\ell_1, N)$ converges pointwise to a limiting distribution which falls off quickly with ℓ_1 ; the nature of this fall off is consistent with the droplet picture as we saw previously. However, we also find that anomalously large loops appear with frequency $O(1/\sqrt{N})$. These large loops have lengths which grow as \sqrt{N} , and their distribution satisfies the following scaling law as $N \rightarrow \infty$

$$\text{Prob}(\tilde{\ell}_1 = x) \sim G(x)/\sqrt{N} \quad (3)$$

with the scaling variable $\tilde{\ell}_1 = \ell_1/\sqrt{N}$. This scaling is illustrated in Figure 2; the finite x contributions at different (large) values of N lead to the same curve $G(x)$. (Note that the fixed size loops lead to a delta function contribution at $x = 0$.) This scaling is incompatible with the droplet picture as can be seen by considering the moments of $P(\ell_1, N)$. If the exponent θ existed, $\rho_\ell(0)$ (and thus $P(\ell_1, N)$) would be $O(\ell^{-2-\theta})$. Then the moments $\langle \ell_1^{1+\delta} \rangle$ would be finite for $\delta < \theta$ and would diverge as $N \rightarrow \infty$ for $\delta > \theta$. However, from Equation 3, the divergence sets in as soon as $\delta > 0$ because of the contribution from the anomalously large loops. The conclusion is that although the droplet picture shows all signs of being correct when one takes the limit $N \rightarrow \infty$ while keeping the scale fixed, it is not valid if one considers scales which grow with the system size!

Mean field picture and energy landscapes — To shed light on these anomalously large loops, consider the mean field picture as obtained by using the properties of the random link MMP. For that model, we have repeated the calculations performed in the Euclidean case and have determined spectra of energies and the sizes of the corresponding excitations. (Although the random link model has been solved by the replica method, this kind of infor-

mation has not been obtained previously.) First of all, we find that all low lying excitations have sizes of $O(\sqrt{N})$. In particular, for the first excited state, we find that the large N scaling is given by $Prob(\tilde{\ell}_1 = x) \sim G_{RL}(x)$, again with $\tilde{\ell}_1 = \ell_1/\sqrt{N}$. The random link model excitations thus have the same \sqrt{N} scaling in size as the anomalous excitations in the Euclidean model, and in fact, the scaling functions $G(x)$ and $G_{RL}(x)$ are qualitatively similar. Note that $G_{RL}(x)$ has no delta function peak at 0, *i.e.*, no contribution from finite size loops; this can be understood from the “geometry” of the random link model: its structure is locally that of a Cayley tree, and as $N \rightarrow \infty$, finite size loops connecting near neighbors disappear. Second of all, we find the following scaling law

$$\langle \mathcal{N}_{RL}(\tilde{E}) \rangle / \Delta \tilde{E} \sim R_{RL}(\tilde{E}) \quad (4)$$

where $\tilde{E} = E\sqrt{N}$ and $\mathcal{N}_{RL}(\tilde{E})$ is the number of loops of (rescaled) energy between \tilde{E} and $\tilde{E} + \Delta \tilde{E}$; the scaling function R_{RL} increases like an exponential.

These results show that the random link MMP has many low-energy large-scale excitations, the characteristic size of which is $O(\sqrt{N})$ and the characteristic energy of which is $O(1/\sqrt{N})$. To obtain a mean field picture for the Euclidean model, we can say that the large scale excitations of the random link model “survive” in the Euclidean model; if we add the small size droplets to these large scale excitations, we generate valleys. (Note that essentially the same droplets make up the different valleys, so that the valleys are nearly identical in structure.) If this picture is correct, we expect the statistics of the excitations associated with the bottom of the valleys of the Euclidean model to be qualitatively similar to the statistics of the states in the random link model. To better see these “valley” states, we have studied the loops of size greater than $C\sqrt{N}$ (where C is a constant). With this restriction, we find that the scaling in size and energy of low energy excitations is very similar in the random link and Euclidean models. In particular, the Euclidean model satisfies Equation 4 with a scaling function R which is close to R_{RL} .

In view of the fact that there is no replica symmetry breaking in the MMP, it may seem surprising to have such a structured landscape; one would expect instead the droplet picture to be the whole story. But this is not the case, the droplet picture breaks down on the scales where the mean field picture predicts large scale excitations of low energy. Since these excitations involve only $O(\sqrt{N})$ bonds, the valleys have an overlap which tends towards one in the $N \rightarrow \infty$ limit, and this is consistent with the absence of replica symmetry breaking. But the point is that these valleys differ by an infinite number of bonds in that limit, and that the droplet picture is valid only within a single valley.

Let us speculate on how our results may extrapolate to the case of the Edwards-Anderson spin glass model.

There may be two types of low energy excitations: the first given by the droplet picture and associated with fixed sizes, and the second given by the mean field picture and associated with system-size excitations involving $O(N)$ spins. This second contribution is responsible for the valleys in the energy landscape. The bottom of the valleys can be thought of as states similar to those arising in the mean field picture, having statistics well described by that approach. In particular, the statistics of the bottom of those valleys may well obey a scaling law such as Equation 4 with $\tilde{E} = EN^\gamma$ where γ is a new exponent; the characteristic inter-level spacing of these valley energies is then $O(N^{-\gamma})$. Of course, the small size droplets give rise to energy levels with a characteristic inter-level spacing of $O(1/N)$. We expect the exponent γ to be given exactly by mean field. We are currently investigating this question.

ACKNOWLEDGMENTS

We are grateful to O. Bohigas, D. Dean and H. Hilhorst for their detailed comments. J.H. acknowledges a fellowship from the MENESR, and O.C.M. acknowledges support from the Institut Universitaire de France. The Division de Physique Théorique is an Unité de Recherche des Universités Paris XI et Paris VI associée au CNRS.

-
- [1] G. Parisi, J. Phys. A **13**, 1101 (1980).
 - [2] D. Sherrington and S. Kirkpatrick, Phys. Rev. Lett. **35**, 1792 (1975).
 - [3] S. F. Edwards and P. W. Anderson, J. Phys. F **5**, 965 (1975).
 - [4] A. J. Bray and M. A. Moore, J. Phys. C Lett. **17**, L463 (1984).
 - [5] W. L. McMillan, Phys. Rev. B **31**, 340 (1985).
 - [6] D. S. Fisher and D. A. Huse, Phys. Rev. B **38**, 386 (1988).
 - [7] C. H. Papadimitriou and K. Steiglitz, *Combinatorial Optimization: Algorithms and Complexity* (Prentice Hall, Englewood Cliffs, NJ, 1982).
 - [8] I. Bieche, R. Maynard, and R. R. J. P. Uhry, J. Phys. A **13**, 2553 (1980).
 - [9] J. Bendisch, Physica A **245**, 560 (1997).
 - [10] M. Mézard and G. Parisi, Europhys. Lett. **2**, 913 (1986).
 - [11] L. Viana and A. J. Bray, J. Phys. C **18**, 3037 (1985).
 - [12] J. Houdayer, J. H. Boutet de Monvel, and O. C. Martin, To appear in Eur. Phys. Jour. B (cond-mat/9803195).
 - [13] P. Grassberger and H. Freund, Z. Oper. Res. **34**, 239 (1990).